Calibration of Polarimetric Automotive Radar with Asymmetric MIMO Topology and Off-Broadside Beamforming

Zhao, Changxu; Garcia-Tejero, Alejandro; Bouwmeester, Wietse; Aslan, Yanki; Krasnov, Oleg; Yarovoy, Alexander

DOI
10.23919/EuRAD61604.2024.10734882

Publication date
2024

Document Version
Final published version

Published in
Proceedings of the 2024 21st European Radar Conference (EuRAD)

Calibration of Polarimetric Automotive Radar With Asymmetric MIMO Topology and Off-Broadside Beamforming

Changxu Zhao[#1], Alejandro Garcia-Tejero[*$2], Wietse Bouwmeester[#3], Yanki Aslan[#4], Oleg Krasnov[#5], Alexander Yarovoy[#6]

[#]Department of Microelectronics, Faculty of EEMCS, TU Delft, The Netherlands
[*]HUBER+SUHNER AG, Switzerland
[$]Universidad Politécnica de Madrid, Spain
{[1]C.Zhao-2, [3]W.Bouwmeester, [4]Y.Aslan, [5]O.A.Krasnov, [6]A.Yarovoy }@tudelft.nl, [2]alejandro.garciatejero@hubersuhner.com

***Abstract* — A far-field calibration method based on broadside measurements with a co-polarized and a cross-polarized reference dihedral target is demonstrated for the first time for an asymmetric $\pm 45^o$ linearly polarized 77 GHz frequency modulated continuous wave (FMCW) multiple-input multiple-output (MIMO) automotive radar. A novel extension of the calibration technique for off-broadside targets' phase response is proposed by using an optimized progressive phase compensation. Rotated dihedral and trihedral targets are used for validation. On broadside, the standard deviation of the channels' phase difference is nearly zero degrees for reference targets and under 5^o for validation targets. The calibration for off-broadside targets shows that the phase relation in the target's scattering matrix can be retrieved, the accuracy of which is dependent on the target's type and angular position.**

***Keywords* — automotive radar, beamforming, calibration, multiple-input multiple-output (MIMO), polarimetry.**

I. Introduction

A polarimetric radar system is able to measure the polarization of the backscattered wave from a target, enabling the retrieval of the target's polarimetric scattering matrix. In the domain of automotive radar, exploiting the target's polarimetric information holds significant potential across diverse applications, including road surface condition recognition [1], multipath separation [2], radar-based point clouds classification [3], and vehicle self-localization [4]. To make use of the many advantages offered by polarimetric radar, it is imperative that the array system is properly calibrated for flexible beamforming.

The calibration of polarimetric radar systems has presented a persistent challenge over the past decades, particularly due to geometric distortion of the polarimetric basis when targets deviate from the broadside direction. This distortion can significantly degrade isolation between co-polarized and cross-polarized channels, resulting in the loss of valuable polarimetric information during target measurement. In [5], the concept of polarimetric bias is used to explain the change in cross-pol level with the target's direction and the method for compensating it using correction matrices was proposed for H-V polarized cross-dipole element. Subsequent research has sought to refine and augment this approach from various aspects such as reduction of the measurement load and extension to different types of radiation elements [6], [7]. Additionally, calibration of a 77 GHz polarimetric radar using the isolated antenna calibration technique (ICAT) was conducted in [8], while the stability of polarimetric information across the target's space was examined in [9]. Despite these advances, current calibration methods for polarimetric radar face limitations on implementation due to the extensive measurement requirements on radiation patterns and neglect of off-broadside beamforming considerations [5], [8]. Moreover, the feasibility and efficacy of applying broadside calibration methods to off-broadside beamforming, as well as their ability to accurately retrieve the target's polarimetric phase response, remain unexplored.

This paper introduces a calibration method utilizing broadside measurements of a co-polarized and cross-polarized reference targets, and introducing, for the first time, optimal progressive phase compensations in off-broadside scenarios. The method is demonstrated, for the first time, on a $\pm 45^o$ linearly polarized 77 GHz radar with asymmetric MIMO topology. A special focus is given on the polarimetric phase response. Off-broadside amplitude changes due to the polarimetric bias is out of the scope of this paper.

The rest of the paper is organized as follows. The design of the radar under test (RUT) is introduced in Section II. The calibration methodology for broadside and off-broadside targets is discussed in Section III. Section IV discusses the measurement flow and calibration results on- and off-broadside. The paper is concluded in Section V.

II. Experimental Polarimetric MIMO RUT

The experimental sensor prototype operates in the 77 GHz band. The RF-front end is based on an AWR2243 MMIC [10] with four receivers, three transmitters, and a metalized plastic waveguide antenna based on a novel 3D printing technique developed by HUBER+SUHNER AG [11] sitting on top of the printed circuit board as depicted in Fig. 1a. The positioning of the physical antenna channels has been selected to reach fully populated arrays at $\lambda_0/2$ distance among the four polarimetric channels, as displayed in Fig. 1b.

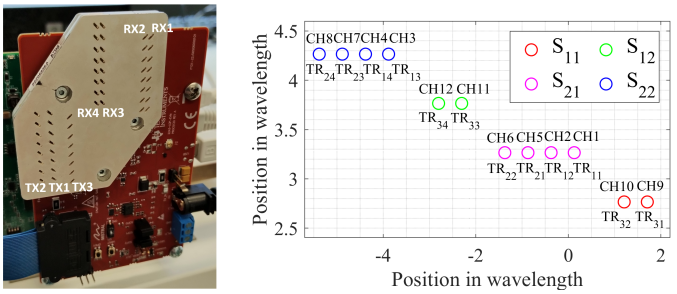

(a) (b)

Fig. 1. Radar under test: (a) MIMO topology; (b) polarimetric virtual array.

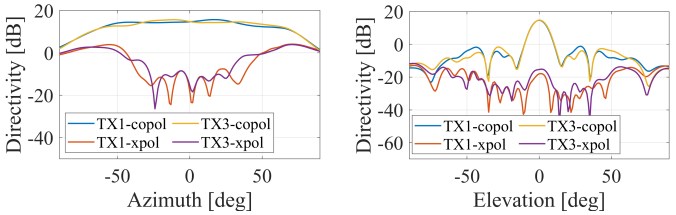

(a) (b)

Fig. 2. TX1 (+45°) and TX3 (-45°) subarray simulated radiation pattern: (a) 0° Elevation cut; (b) 0° Azimuth cut.

Two types of subarrays with orthogonal slant (±45°) polarizations have been employed for pattern similarity. Their design is based on a linear array of eight open waveguides [12]. Fig. 2 shows the simulated radiation performance of both antenna types, achieving an elevation 3-dB field-of-view (FOV) of 9.1° and azimuth of 105°. Furthermore, a level of cross-polarization isolation of 35 dB is obtained at boresight, reducing to 5 dB at 60° in the azimuthal plane.

III. Calibration Methodology

A. Calibration On Broadside

According to the IACT method [13], the polarimetric RUT's broadside calibration uses measurements from two reference targets with known scattering matrices: one for co-polarized channels and one for cross-polarized channels. A similar approach has been adapted here using a rotatable dihedral to calculate the calibration matrix. The angular-dependent scattering properties of the dihedral corner reflector are described by its scattering matrix $S_{DH}(\alpha)$ in (1), where α represents the rotation angle and σ_{DH} denotes its radar cross-section. For the $\pm 45^o$ polarization basis, the 0° rotated dihedral is chosen as the cross-polarization target, while the 45° rotated dihedral serves as the co-polarization target. Calibration variables are obtained by calculating the ratio between the reference channels and others for co-polarized and cross-polarized channels, respectively. The trihedral was then selected as one of the validation targets with scattering matrix S_{TH} in (1), where σ_{TH} indicates its radar cross-section.

$$S_{DH}(\alpha) = \sqrt{\tfrac{\sigma_{DH}}{4\pi}} \begin{bmatrix} -\cos 2\alpha & \sin 2\alpha \\ \sin 2\alpha & \cos 2\alpha \end{bmatrix} \quad S_{TH} = \sqrt{\tfrac{\sigma_{TH}}{4\pi}} \begin{bmatrix} 1 & 0 \\ 0 & 1 \end{bmatrix} \quad (1)$$

The calibration process begins with selecting reference channels for both cross-polarized and co-polarized channels. In this study, channels 3 and 1 are chosen for co-polarized and cross-polarized channels, respectively (see Fig. 1b). Calibration parameters for co-polarized channels are derived using measurements from the 45° rotated dihedral, as outlined in (2). Here, CH_i represents the measured data from the range bin where the target is located after range compression, and the additional 180° phase shift induced by the scattering matrix of the 45° rotated dihedral is compensated for by the term $e^{-j\pi}$. Similarly, calibration parameters for cross-polarized channels can be computed using (3), utilizing the measurement outcomes from the 0° rotated dihedral. To combine the two distinct calibration matrices, C_{co} and C_{cross}, into a unified entity, the ratio between the measurement results of the co- and cross-polarized reference channels is calculated as demonstrated in (4). With R_{ref}, the two calibration matrices were merged into a single diagonal matrix, and its diagonal entries are delineated in (5) in the channel order.

$$C_{\text{co,diag}} = (1, \tfrac{CH_3}{CH_4}, \tfrac{CH_3}{CH_7}, \tfrac{CH_3}{CH_8}, \tfrac{CH_3}{CH_9} \cdot e^{-j\pi}, \tfrac{CH_3}{CH_{10}} \cdot e^{-j\pi}) \quad (2)$$

$$C_{\text{cross,diag}} = (1, \tfrac{CH_1}{CH_2}, \tfrac{CH_1}{CH_5}, \tfrac{CH_1}{CH_6}, \tfrac{CH_1}{CH_{11}}, \tfrac{CH_1}{CH_{12}}) \quad (3)$$

$$R_{\text{ref}} = \frac{CH_1}{CH_3} \quad (4)$$

$$\begin{aligned} C_{\text{tot,diag}} = (&1, \tfrac{CH_1}{CH_2}, R_{\text{ref}}, \tfrac{CH_3}{CH_4} \cdot R_{\text{ref}}, \tfrac{CH_1}{CH_5}, \tfrac{CH_1}{CH_6}, \tfrac{CH_3}{CH_7} \cdot R_{\text{ref}} \ldots \\ &\ldots \tfrac{CH_3}{CH_8} \cdot R_{\text{ref}}, \tfrac{CH_3}{CH_9} \cdot e^{-j\pi} \cdot R_{\text{ref}}, \tfrac{CH_3}{CH_{10}} \cdot e^{-j\pi} \cdot R_{\text{ref}} \ldots \\ &\ldots \tfrac{CH_1}{CH_{11}}, \tfrac{CH_1}{CH_{12}}) \end{aligned} \quad (5)$$

B. Calibration Off-Broadside

The polarimetric bias, stemming from geometrical distortions of the polarimetric basis when the target is situated off-broadside, will alter the ratio of co-pol to cross-pol in the received waveform. Compensating those biases for the radar and targets under test [5] is out of the scope of this paper. Here, a novel off-broadside calibration technique is proposed to recover the phase response of the targets.

When the target is positioned off-broadside, a progressive phase shift Φ_{prog} arises among the virtual array elements due to the new angle-of-arrival (Φ_{AOA}). If the target is in the far-field and located in 0° elevation angle, the vertical distribution of the virtual array shown in Fig. 1b can be disregarded. Hence, the virtual array layout can be simplified by assuming that the virtual array elements are positioned without vertical separation. This simplification yields the same phase response as the original layout.

Calibrating for off-broadside beamforming can be achieved by implementing the same calibration method as for broadside, followed by compensating for the progressive phase shift using (6), where d indicates the spacing between virtual array elements, c is the speed of light and f_c is the radar operational frequency. This phase compensation entails designating a reference channel (CH1 here) and subsequently compensating for the progressive phase differences on other channels relative to the reference channel.

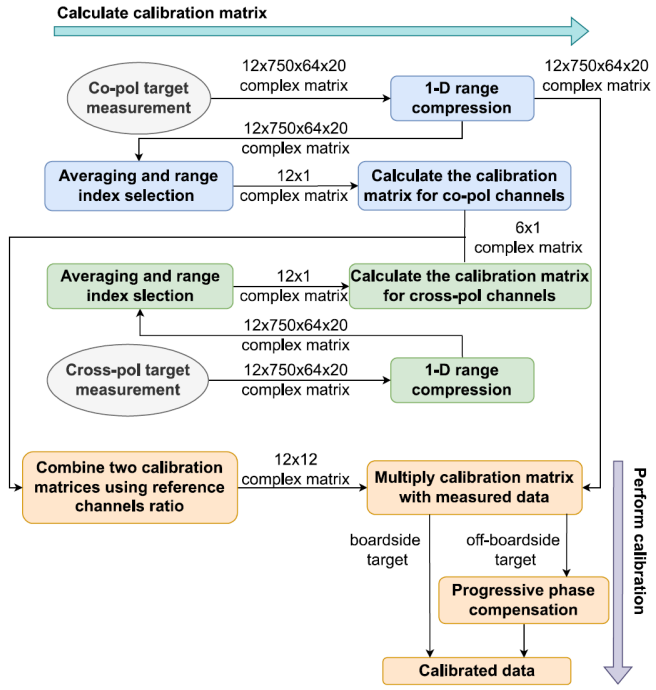

Fig. 3. Flowchart of the calibration process.

$$\Phi_{\text{prog}} = \sin\Phi_{\text{AOA}} \cdot \frac{d}{c} \cdot 2\pi f_c \tag{6}$$

IV. Measurement Results

A. Measurement Setup and Data Processing Flow

The measurements were performed in the anechoic chamber of TU Delft. The measured targets were a rotatable dihedral and a trihedral. The size of the reflectors are larger than 10 wavelengths at 77 GHz and the distance between the RUT and the reflectors was set to 3.6 m. During the off-broadside measurement, the targets were always facing the RUT.

The raw measurement data consists of a 12x750x64x20 complex 4-D matrix, where 12 represents the number of channels, 750 is the number of samples per chirp, 64 denotes the number of chirps per frame, and 20 signifies the number of frames. The process flow for the calibration is depicted in Fig. 3, where the implementation of the calibration matrix is shown for the co-pol target as an example. In this study, the angle of arrival employed for phase compensation for off-broadside calibration was optimized after a fast search around the true target direction, resulting in the best match with the phase response of the target scattering matrix.

B. On-Broadside Calibration Results

The $0°$ and $45°$ rotated dihedrals were used as the reference target for calibration while the $67.5°$ rotated dihedral and the trihedral were used for validation purposes. The results for broadside measurement are shown in Table 1, where A stands for the amplitude (normalized for the overall maximum, i.e. DH45 on broadside), $|\Phi_{+45+45} - \Phi_{-45-45}|$ stands for phase difference between $(+45^o, +45^o)$ and $(-45^o, -45^o)$ co-polarized channels, $|\Phi_{+45-45} - \Phi_{-45+45}|$ stands for phase difference between $(+45^o, -45^o)$ and $(-45^o, +45^o)$ cross-polarized channels, and s.t.d. stands for the standard deviation. The phase and amplitude distribution of the calibration targets is shown in Fig. 4 and Fig. 5, while Fig. 6 shows these for validation targets.

After the calibration, the mean phase difference between the co- and cross-polarized channels of the two reference targets: $45°$ rotated dihedral and the $0°$ rotated dihedral, reached -180^o and nearly zero degrees respectively. Conversely, the validation results from the $67.5°$ rotated dihedral indicate that the co-polar channels' phase difference reaches 181.5^o as expected. At the same time, the s.t.d. is maintained at 0.6^o and 3^o for co-polar and cross-polar channels, respectively. Furthermore, the validation results for the trihedral exhibit an s.t.d. of $4.3°$ for the co-polar channels' phase difference. An expected increment in the s.t.d. of phase difference is observed when the target is changed from the reference dihedral to the non-reference targets. However, this is still acceptable compared to [8].

C. Off-Broadside Calibration Results

The results of the off-broadside beamforming calibration are shown in Table 2. The phase and amplitude distribution of the calibrated results are shown in Fig. 7 and Fig. 8. The measurement of the $67.5°$ rotated dihedral at $30°$ azimuth shows that after the calibration for off-broadside beamforming, the phase difference between co-polar channels is 184.1^o, which is well-matched with its scattering matrix. For the measurement of the 0^o rotated dihedral from 30^o to 60^o in azimuth, the s.t.d. of the cross-polar channels' phase difference

Table 1. Calibration results in broadside.

co-pol target / x-pol target / dual-pol target	<A> [dB]	$\lvert\phi_{+45+45} - \phi_{-45-45}\rvert$ [deg]		$\lvert\phi_{+45-45} - \phi_{-45+45}\rvert$ [deg]	
	Norm.	Mean	S.t.d	Mean	S.t.d
DH 45°	0	125	132.5	/	/
DH 45° calibrated	-1.1	-180	0	/	/
TH calibrated	-8.6	18	4.3	/	/
DH 0°	-0.6	/	/	97.4	63.7
DH 0° calibrated	-1.1	/	/	0	0
DH 67.5° calibrated	-5.5	-181.5	0.6	-18.8	3

Table 2. Calibration results for off-broadside beamforming.

co-pol target / x-pol target / dual-pol target	Tru. Φ_{AOA} / Est. Φ_{AOA} [deg]	<A> [dB]	$\lvert\phi_{+45+45} - \phi_{-45-45}\rvert$ [deg]		$\lvert\phi_{+45-45} - \phi_{-45+45}\rvert$ [deg]	
		Norm.	Mean	S.t.d	Mean	S.t.d
DH 0°, 30° azi	30/30	-4.2	/	/	-4.9	4.2
DH 0°, 60° azi	60/60	-8.1	/	/	-0.4	5.9
TH, 30° azi	30/31.8	-11	-0.04	4.4	/	/
TH, 60° azi	60/65.5	-14.5	-2	1.4	/	/
DH 67.5°, 30° azi	30/32	-9.6	184.1	6	-43.3	3.5

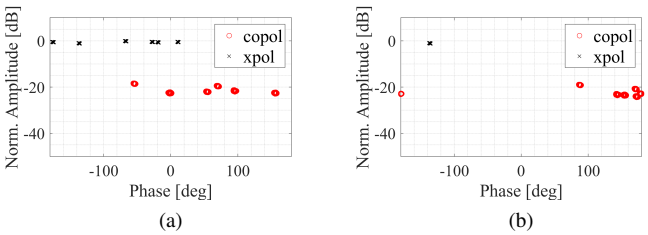

Fig. 4. Broadside calibration with $0°$ dihedral: (a) uncalibrated; (b) calibrated.

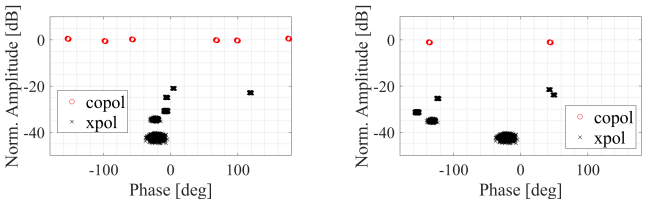

Fig. 5. 45° dihedral in broadside: (a) uncalibrated; (b) calibrated.

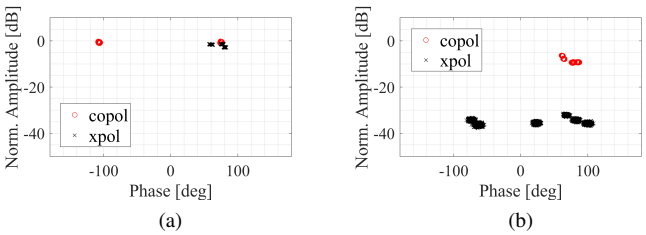

Fig. 6. Calibrated broadside measurement: (a) 67.5° dihedral; (b) trihedral.

increased 1.7^o and the average amplitude dropped 3.9 dB. In addition, the s.t.d. of channel phase difference varies on validation targets as shown on the 67.5^o rotated dihedral and trihedral in different azimuth angles. Moreover, 1.8°, 5.5° and 2° angular error between the target's true Φ_{AOA} and the Φ_{AOA} used for phase compensation were found in the results from the trihedral and the 67.5° rotated dihedral. Despite some angular error being observed, it is still sufficient to distinguish between different off-broadside targets based on the retrieved phase relation in the target's scattering matrix.

V. Conclusion

A far-field calibration method based on broadside measurements with a rotated dihedral as the reference target is demonstrated for an asymmetric $\pm 45^o$ polarized 77 GHz MIMO FMCW automotive radar. An optimized progressive phase compensation technique is proposed for off-broadside calibration on the target's phase response. The broadside measurements show the s.t.d. of the channel phase difference around 0^o for the reference targets and under 5^o for the validation targets. The calibration for off-broadside 67.5^o rotated dihedral accurately retrieves the 180^o phase relation between the co-pol and cross-pol channels, which is well-matched with the target's scattering matrix. The accuracy of the calibration on the targets' phase response is found to be dependent on the target's type and angular position, which raises the s.t.d. of the phase for the dihedral and decreases it for the trihedral when moving off-broadside. The proposed calibration method is adaptable to radars with different numbers of channels and element positions, as well as to targets at various elevation angles. This flexibility makes it a valuable tool for enhancing the study of polarimetric MIMO automotive radar calibration in non-broadside scenarios.

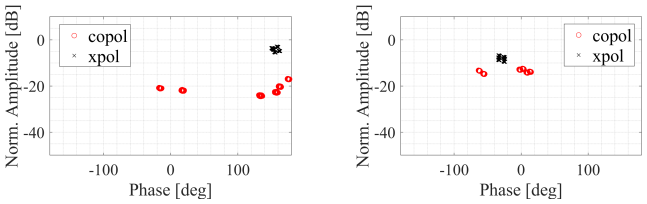

Fig. 7. Off-broadside calibrated results of the 0° dihedral: (a) 30° azimuth; (b) 60° azimuth.

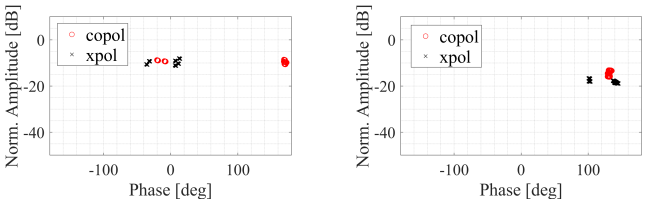

Fig. 8. Calibrated off-broadside beamforming results: (a) 67.5° dihedral in 30° azimuth; (b) trihedral in 60° azimuth.

References

[1] W. Bouwmeester, F. Fioranelli, and A. G. Yarovoy, "Road surface conditions identification via h α a decomposition and its application to mm-wave automotive radar," *IEEE Transactions on Radar Systems*, vol. 1, pp. 132–145, 2023.

[2] T. Visentin, J. Hasch, and T. Zwick, "Analysis of multipath and DOA detection using a fully polarimetric automotive radar," in *European Radar Conference*, Oct. 2017, pp. 45–48.

[3] J. F. Tilly, O. Schumann, F. Weishaupt, J. Dickmann, and G. Waniliek, "Polarimetric Information Representation for Radar based Road User Detection with Deep Learning," in *IEEE International Conference on Information Fusion*, Nov. 2021, pp. 1–6.

[4] F. Weishaupt, K. Werber, J. Tilly, J. Dickmann, and D. Heberling, "Polarimetric Radar for Automotive Self-Localization," in *International Radar Symposium*, Jun. 2019, pp. 1–8.

[5] G. Zhang, R. J. Doviak, D. S. Zrnic, J. Crain, D. Staiman, and Y. Al-Rashid, "Phased Array Radar Polarimetry for Weather Sensing: A Theoretical Formulation for Bias Corrections," *IEEE Trans Geosci Remote Sens*, vol. 47, no. 11, pp. 3679–3689, Nov. 2009.

[6] J. Zhou, C. Pang, Y. Wang, Z. Wang, Y. Li, and X. Wang, "An Efficient Bias Correction Method for Large Planar Polarimetric Phased Array Radar," *IEEE Antennas Wirel Propag Lett*, vol. 22, no. 8, pp. 1778–1782, Aug. 2023.

[7] L. Lei, G. Zhang, and R. J. Doviak, "Bias Correction for Polarimetric Phased-Array Radar With Idealized Aperture and Patch Antenna Elements," *IEEE Trans Geosci Remote Sens*, vol. 51, no. 1, pp. 473–486, Jan. 2013.

[8] T. Visentin, J. Hasch, and T. Zwick, "Calibration of a fully polarimetric 8×8 mimo fmcw radar system at 77 ghz," in *European Conference on Antennas and Propagation*, Mar. 2017, pp. 2530–2534.

[9] F. Weishaupt, J. F. Tilly, N. Appenrodt, J. Dickmann, and D. Heberling, "Calibration and Signal Processing of Polarimetric Radar Data in Automotive Applications," in *Mediterr. Microw. Symp.*, May 2022, pp. 1–6.

[10] B. P. Ginsburg, K. Subburaj, S. Samala, *et al.*, "A multimode 76-to-81ghz automotive radar transceiver with autonomous monitoring," in *2018 IEEE International Solid - State Circuits Conference - (ISSCC)*, 2018, pp. 158–160.

[11] U. Huegel, A. Garcia-Tejero, R. Glogowski, E. Willmann, M. Pieper, and F. Merli, "3D waveguide metallized plastic antennas aim to revolutionize automotive radar.," *Microwave Journal*, vol. 65, no. 9, 2022.

[12] A. Garcia-Tejero, M. Burgos-Garcia, and F. Merli, "High-efficiency injection-molded waveguide horn antenna array for 76-81 ghz automotive radar applications," in *2022 19th European Radar Conference (EuRAD)*, 2022, pp. 21–24.

[13] K. Sarabandi, F. Ulaby, and M. Tassoudji, "Calibration of polarimetric radar systems with good polarization isolation," *IEEE Transactions on Geoscience and Remote Sensing*, vol. 28, no. 1, pp. 70–75, 1990. DOI: 10.1109/36.45747.